Novel Type of Ohmic Contacts to P-Doped GaN Using Polarization Fields in Thin $In_xGa_{1-x}N$ Capping Layers

Th. GESSMANN,[1] Y.-L. LI,[1] E.L. WALDRON,[2] J.W. GRAFF,[1] E.F. SCHUBERT,[1] and J.K. SHEU[3]

1.—Department of Electrical and Computer Engineering, Boston University, Boston, MA 02215. 2.—Department of Electrical and Computer Engineering and Department of Physics, Boston University, Boston, MA 02215. 3.—Optical Science Center, National Central University, Chung-Li 32054, Taiwan, Republic of China

Thin p-doped InGaN layers on p-doped GaN were successfully used to demonstrate a new type of low-resistance ohmic contact. A significant reduction of specific contact resistance can be achieved by increasing the free-hole concentration and the probability for hole tunneling through the Schottky barrier as a consequence of polarization-induced band bending. As obtained from the transmission-line method, the specific contact resistances of Ni (10 nm)/Au (30 nm) contacts deposited on InGaN capping layers were 1.2×10^{-2} Ωcm^2 and 6×10^{-3} Ωcm^2 for capping layer thicknesses of 20 nm and 2 nm, respectively.

Key words: InGaN, GaN, p-doping, polarization, specific contact resistance, ohmic contact

INTRODUCTION

The performance of devices fabricated from GaN and related compounds is strongly affected by the resistances caused by electrical contacts. To avoid excessive heating resulting in a failure of the device, specific contact resistances less than $\sim 10^{-3}$ Ωcm^2 for light-emitting diodes (LEDs) and less than $\sim 10^{-4}$ Ωcm^2 for laser diodes are required.[1] This applies in particular to ohmic contacts on p-doped GaN (p-GaN) due to the resistive nature of GaN obtained by standard p-type doping techniques.[1,2]

Several methods have been used to attain low, specific contact resistances to p-GaN, such as deposition of high work-function metals,[3] growth of AlGaN/GaN superlattices,[4,5] and tunnel-diode structures on top of p-GaN.[6]

In this publication, the use of thin $In_xGa_{1-x}N$ capping layers, pseudomorphically grown on top of p-doped GaN, is presented. Strain-induced piezoelectric as well as spontaneous polarization fields in the InGaN capping layer and the lower p-GaN layer cause band bending that leads to the formation of a two-dimensional (2-D) hole gas (HG).[7] As a result, the concentration of free holes at the InGaN/GaN interface is greatly increased, and the tunneling barrier width of the metal-semiconductor contact is reduced, thereby allowing for a high hole-tunneling probability through the barrier. The theory describing ohmic contacts to p-GaN by using thin $In_xGa_{1-x}N$ capping layers will be presented together with experimental results, demonstrating the capability of the new approach in achieving low contact resistances.

(Received October 11, 2001; accepted February 1, 2002)

EXPERIMENTAL

The samples were grown by metal-organic chemical vapor deposition along the c direction on top of single-crystalline sapphire substrates. The grown structures consist of a 4-μm-thick n-doped GaN layer; a 5-pair multiquantum-well LED, with barrier/well widths of 7.5 nm/2.5 nm, respectively; a 20-nm $Al_{0.15}Ga_{0.85}N$ electron blocking layer; a 130-nm-thick p-doped, GaN upper-cladding layer; and a p-doped $In_{0.27}Ga_{0.73}N$ capping layer that is either 2-nm or 20-nm thick. The two layers were Mg-doped to a concentration of about $N_{Mg} = 3 \times 10^{18}$ cm^{-3} as determined from capacitance-voltage measurements. The quality of the sample surfaces was checked by Nomarski microscopy; no indications of islanding could be found.

The Ni (10 nm)/Au (30 nm) contacts were deposited by electron-beam evaporation using lift-off photolithographic techniques. The contacts were

square-shaped pads (180 μm × 180 μm) separated by 2-μm, 4-μm, 6-μm, 8-μm, 10-μm, and 15-μm wide gaps. To remove surface oxide layers, the samples were dipped in a buffered-oxide etch solution for 3 min prior to mounting them in the deposition chamber. Subsequently, the contacts were annealed for 3 min in a rapid thermal annealing furnace at 500°C in an oxygen ambient. The contact resistances were determined from current-voltage (*I-V*) measurements using the transfer length method (TLM).

RESULTS AND DISCUSSION

The piezoelectric polarization, P_{pz}, and the spontaneous polarization, P_{sp}, in the $In_xGa_{1-x}N$ capping layer due to biaxial strain and in the absence of external electric fields depend on the In content, x, as depicted in Fig. 1a. The piezoelectric polarization can be calculated from

$$P_{pz}(x) = 2 \times \frac{a_{0,GaN} - a_0}{a_0}\left(e_{31} - e_{33}\frac{C_{13}}{C_{33}}\right) \quad (1)$$

with the piezoelectric coefficients, e_{31} and e_{33}; the bulk moduli, C_{13} and C_{33}; and the equilibrium lattice constant, a_0, in the basal plane of the Wurtzite structure (Table I). In Eq. 1, the quantity $a_{0,GaN}$ corresponds to the lattice constant of the pseudomorphically grown, capping layer. The values of the spontaneous polarizations in the capping layer and the relaxed-GaN layer, P_{sp} and $P_{sp,GaN}$, are listed in Table I as well. The terms P_{sp} and $P_{sp,GaN}$ are negative because the two vectors, $\boldsymbol{P}_{sp}$ and $\boldsymbol{P}_{sp,GaN}$, point toward the substrate, i.e., in the negative c direction for Ga-faced samples.

Figure 1a also shows the x dependence of the sheet-charge densities at the surface and at the InGaN/GaN interface given by

$$\sigma_s(x) = P_{pz} + P_{sp}, \text{ and } \sigma_i(x) = P_{sp,GaN} - (P_{pz} + P_{sp}) \quad (2)$$

respectively.

The electrical fields in the capping layer, $\boldsymbol{\mathcal{E}}_{pz}$ and $\boldsymbol{\mathcal{E}}_{sp}$, can be calculated from the corresponding polarization fields, P_{pz} and P_{sp}, using the relative dielectric permeability $\varepsilon_{InGaN}(x) = 10.4 + 3.9 \times x$ (Fig. 1b). If $\boldsymbol{\mathcal{E}}_{sp,GaN}$ denotes the electric field caused by the spontaneous polarization, $P_{sp,GaN}$, in the relaxed-GaN layer, the corresponding field in the capping layer is given by $-\boldsymbol{\mathcal{E}}_{sp,GaN}$ due to the change of sign when crossing the interface.

Figure 2 shows the band diagram of an elastically strained, 20-nm-thick, p-doped $In_{0.27}Ga_{0.73}N$ capping layer on top of relaxed p-GaN, self-consistently calculated for T = 300 K by solving the coupled Schrödinger and Poisson equations in one dimension.[9] We assumed a uniform Mg-dopant concentration of $N_{Mg} = 10^{19}$ cm^{-3} with an acceptor activation energy of E_a = 272 meV in the capping layer as obtained from linear extrapolation using E_a = 170 meV for p-GaN and E_a = 204 meV for p-$In_{0.09}Ga_{0.91}N$.[10] It should be noted, however, that E_a is not a strong parameter, and changing the activation energies within about 50 meV does not substantially alter the results. In order to include the polarization-induced sheet-charge densities in the band calculation, 0.1-nm-thick layers were added at the surface and at the $In_{0.27}Ga_{0.73}N$/GaN interface, containing volume charge densities of 1.26 × 10^8

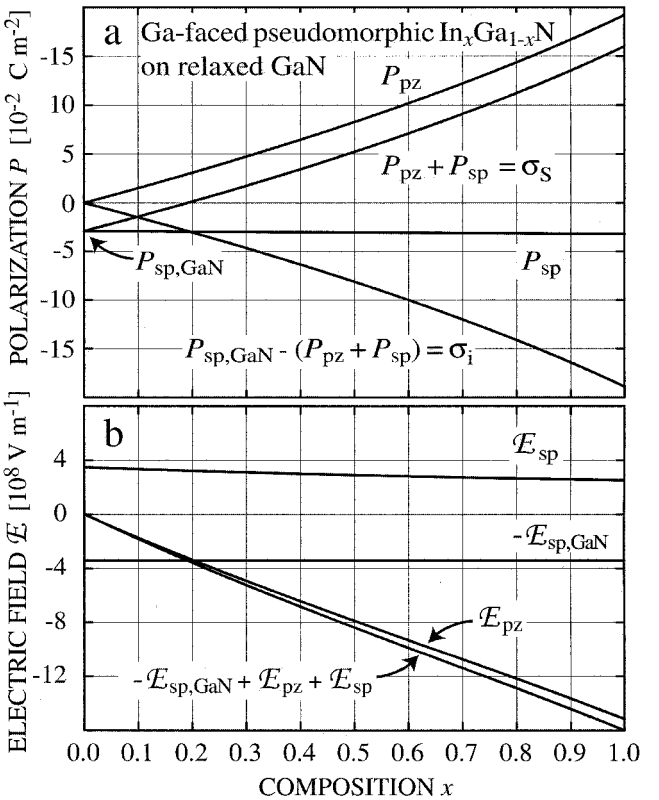

Fig. 1. (a) Spontaneous and piezoelectric polarizations, P_{sp} and P_{pz}, in a pseudomorphically strained $In_xGa_{1-x}N$ capping layer depending on the In concentration, x. The curves were calculated using Eq. 1 and the values listed in Table I; surface and interface charge densities, σ_s and σ_i, were calculated from Eq. 2. (b) The electric fields, $\boldsymbol{\mathcal{E}}_{sp}$ and $\boldsymbol{\mathcal{E}}_{pz}$, in the $In_xGa_{1-x}N$ capping layer obtained from P_{sp} and P_{pz}. Note that the field $\boldsymbol{\mathcal{E}}_{sp,GaN}$ in the relaxed-GaN layer results in a contribution $-\boldsymbol{\mathcal{E}}_{sp,GaN}$ in the capping layer.

Table I. Piezoelectric Coefficients, e_{11} and e_{13}; Bulk Moduli, C_{11} and C_{13}, Spontaneous Polarization P_{sp}, and Lattice Constant A_0 of Wurtzite GaN, InN, and $In_xGa_{1-x}N$ The Data were Taken from Ref. 8 and Used to Calculate the Curves in Fig. 1

	e_{31} (C m^{-2})	e_{33} (C m^{-2})	C_{13} (GPa)	C_{33} (GPa)	P_{sp} (cm^{-2})	a_0 (10^{-10} m)
GaN	−0.49	0.73	103	405	−0.029	3.189
InN	−0.57	0.97	92	224	−0.032	3.54
$In_xGa_{1-x}N$	−0.08 x − −0.49	0.24 x + +0.73	−11 x + +103	−181 x + +405	−0.003 x + −0.029	0.351 x + +3.189

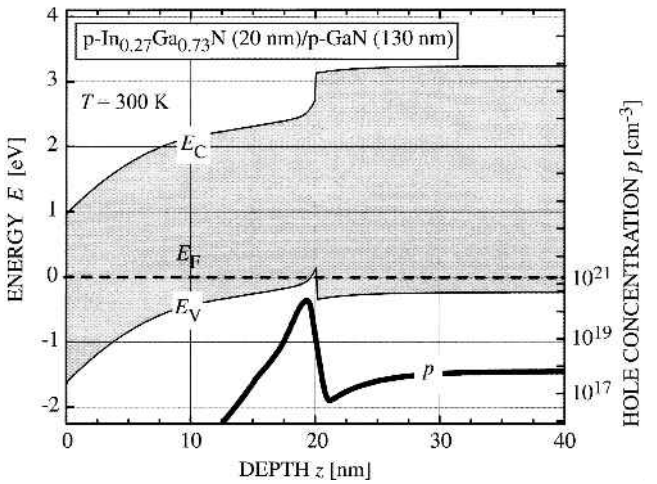

Fig. 2. Self-consistently calculated, band diagram and hole concentration, p, of a 20-nm-thick p-doped $In_{0.27}Ga_{0.73}N$ layer grown pseudomorphically on p-doped GaN with a dopant concentration of 10^{19} cm^{-3}.

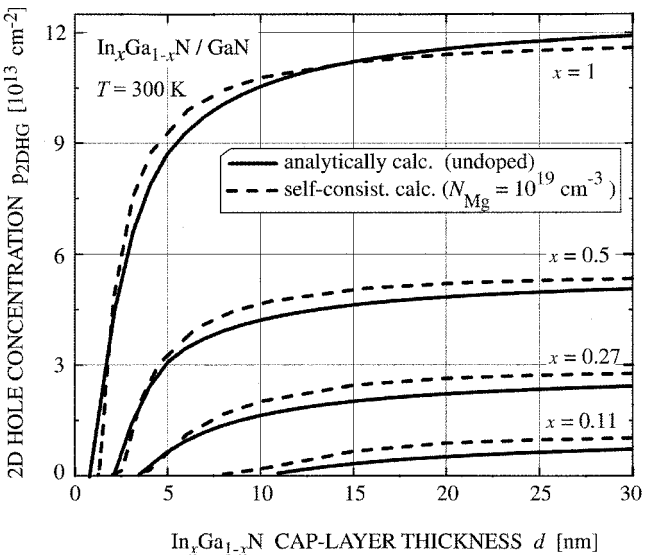

Fig. 3. Dependence of the 2-D HG density, p_{2DHG}, on the InGaN capping-layer thickness, d, calculated for different In contents, *x*. The solid lines are numerical solutions of Eq. 3. The values of the dashed curves are the integrals of the hole concentration, *p*, over the peak region at different *x* and *d* (Fig. 2 shows $x = 0.27$ and $d = 20$ nm).

C m^{-3} and -4.2×10^8 C m^{-3}, respectively, that correspond to $\sigma_s = 1.26 \times 10^{-2}$ C m^{-2} and $\sigma_i = -4.2 \times 10^{-2}$ C m^{-2} at $x = 0.27$. Figure 2 also includes the calculated depth dependence of the hole concentration, p.

It is evident that the strong band bending in the $In_{0.27}Ga_{0.73}N$ capping layer, induced by the polarization fields, results in a peak of the hole distribution close to the InGaN/GaN interface, indicating the formation of a two-dimensional (2-D) hole gas (HG).

Figure 3 shows the 2-D HG density, p_{2DHG}, as a function of the thickness, d, and the In content, x, of the InGaN capping layer. The values for p_{2DHG} were calculated by integrating over the peak region of the hole concentration, p, for different d and x (Fig. 2 shows $x = 0.27$ and $d = 20$ nm) or by numerically solving the equation of energy conservation for a hole moving in c direction through the InGaN capping layer.

$$eF_B + ed\mathcal{E}_{tot} + (E_0 - E_V) + (E_F - E_0) = 0 \quad (3)$$

In Eq. 3, d denotes the thickness of the capping layer, e is the elementary charge, $\mathcal{E}_{tot}$ is the total electric field in the capping layer, Φ_B is the Schottky barrier height, E_V is the valence band energy, and E_F and E_0 are the Fermi energy and the energy of the 2-D HG ground state, respectively. The different contributions to the left-hand side in Eq. 3 are given by

$$e\Phi_B = E_{G,InGaN} - e(\Phi_M - \chi_{InGaN}) \quad (4a)$$

$$\mathcal{E}_{tot} = -\mathcal{E}_{Sp,GaN} + \mathcal{E}_{Sp,InGaN} + \mathcal{E}_{pz,InGaN} + \frac{ep_{2DHG}}{\varepsilon_{InGaN}\varepsilon_0} \quad (4b)$$

$$E_0 - E_V = \frac{3}{2}\left[\frac{3}{2}\frac{e^2\hbar}{\varepsilon_{InGaN}\varepsilon_0\sqrt{m^*}}p_{2DHG}\right]^{2/3} \quad (4c)$$

$$E_F - E_0 = \frac{\pi\hbar^2}{m^*}p_{2DHG} \quad (4d)$$

$E_{G,InGaN}$ and χ_{InGaN} in Eq. 4a are the bandgap and the electron affinity of the $In_xGa_{1-x}N$ capping layer, Φ_M is the work function of the contact metal, and ε_0 denotes the dielectric permittivity in a vacuum; here, we used the work function of Ni, $\Phi_M = 5.2$ eV. The bandgap energy was obtained from

$$E_{G,InGaN} = (1-x)E_{G,GaN} + xE_{G,InN} - bx(1-x) \quad (5)$$

with $E_{G,InN} = 1.9$ eV, $E_{G,GaN} = 3.45$ eV, and the bowing parameter $b = 2.5$ eV.[8] Using the electron affinities of InN and GaN, $\chi_{InN} = 4.5$ eV[11] and $\chi_{GaN} = 4.1$ eV.[11] The dependence of χ_{InGaN} on the In concentration, x, can be calculated according to

$$\chi_{InGaN} = \chi 4.5\text{ eV} + (1-x)4.1\text{ eV} \quad (6)$$

In Eq. 4c, $E_0 - E_V$ was obtained from the Fang-Howard approximation[12] for energy states in a triangular well. The effective hole mass, m^*, is taken to be equal to the free-electron mass, m_0, and $\hbar$ is Planck's constant divided by 2π. The $E_F - E_0$ in Eq. 4d was calculated using the high-density approximation of the Fermi-Dirac distribution and the 2-D density of hole states $\rho_{2D} = m^*/(\pi\hbar^2)$. Comparison of the analytical results with the self-consistently calculated results shown in Fig. 3 reveals good agreement. Minor differences can be attributed to differences in doping concentration.

The *I-V* characteristics of the contacts to both $In_{0.27}Ga_{0.73}N$ capping layers are linear for all the contact-pad separations (Fig. 4). However, at the same voltages, the current through the thick capping layer is about one order of magnitude smaller compared to the thin capping layer.

The pad-to-pad resistances calculated from the *I-V* data for different pad separations are shown in Fig. 5, together with the results of the TLM analysis of these data. The specific contact resistance, $\rho_c = 6 \times 10^{-3}$ Ωcm^2 for the 2-nm capping layer, is smaller by a factor of 2 than $\rho_c = 1.2 \times 10^{-2}$ Ωcm^2 for the 20-nm layer.* According to the Wentzel–Kramers– Brillouin approximation, the one-dimensional, hole-tunneling probability, T_z, along the z direction through a semiconducting layer of width d can be written as

$$T_z = \exp\left[-\int_0^d 2h^{-1}\sqrt{2m^* E_v(z)}\,dz\right] \quad (7)$$

The tunneling probability, T_z, in Eq. 7 increases exponentially upon decreasing the layer thickness, *d*. Thin capping layers are, therefore, preferable in order to increase the hole transport through the barrier and to lower the contact resistance,[13] even though the 2-D HG density vanishes for sufficiently thin layers (Fig. 2).

* Measurements on p-doped GaN reference samples with the same contacts annealed at 500°C yielded contact resistances in the 10^{-3} Ωcm^2 range and are, thus, comparable to our present results. Based on theoretical and recent experimental results,[4,13] further optimization of the polarization enhanced contacts is expected to reduce the contact resistance.

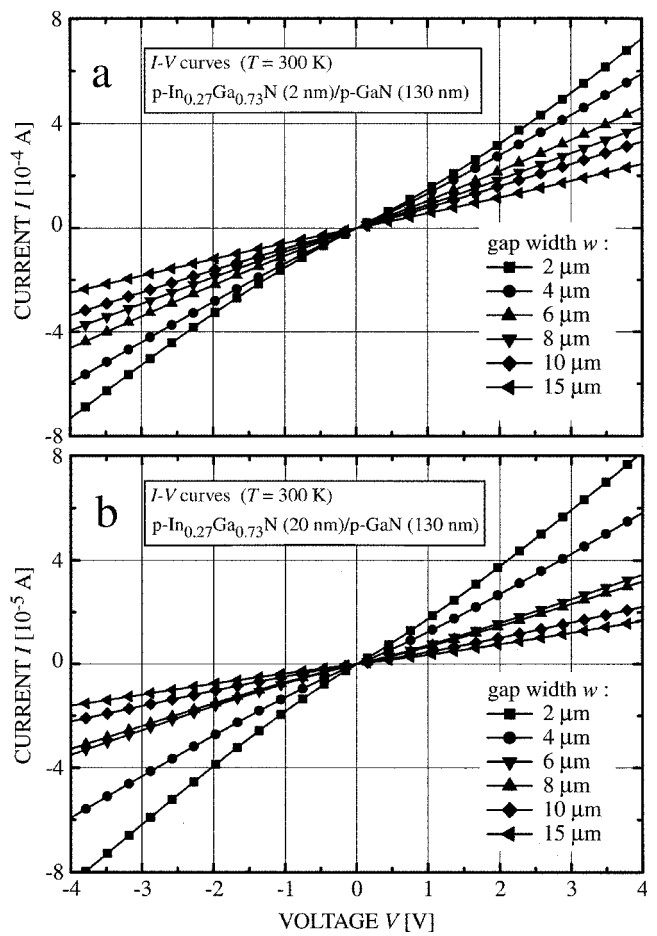

Fig. 4. Current-voltage curves measured on InGaN/GaN samples with (a) a 2-nm-thick and (b) a 20-nm-thick $In_{0.27}Ga_{0.73}N$ capping layer.

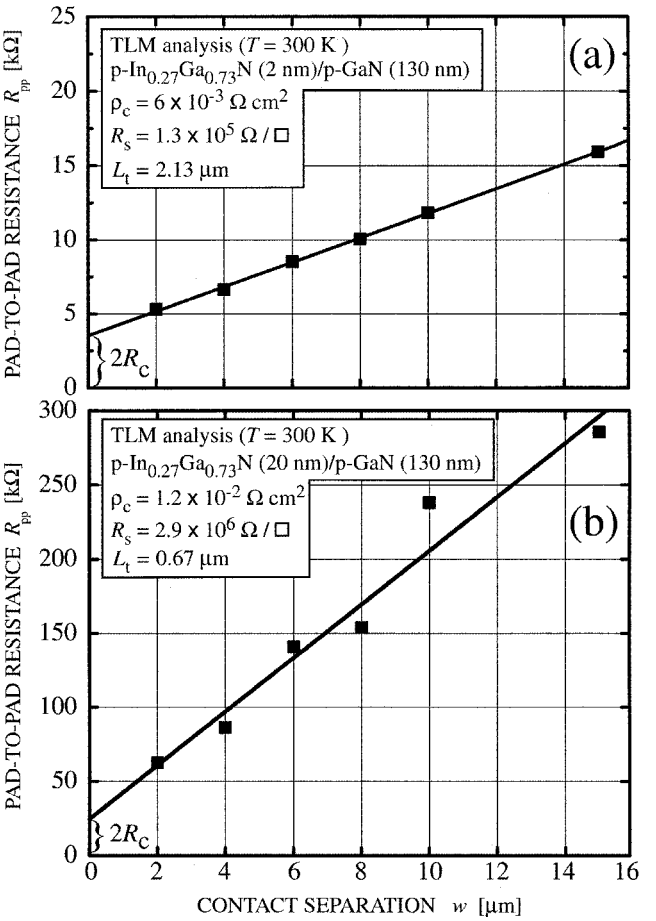

Fig. 5. Pad-to-pad resistances, R_{pp}, obtained from the *I-V* curves in Fig. 4. The solid lines are straight line fits to the data analyzed using the TLM model. The values obtained for the specific contact resistance, ρ_c, the sheet resistance, R_s, and the transfer length, L_t, are shown in the insets.

By reducing the thickness of the InGaN capping layer from 20 nm to 2 nm, however, the contact resistance changed only by a factor of 0.5; this might indicate limitations to the hole transport not taken into account by Eq. 7, possibly caused by defects, such as dislocations in the InGaN capping layers or by approaching the critical thickness in the 20-nm-thick capping layer.

CONCLUSIONS

In conclusion, we have shown a method using the polarization in thin-InGaN capping layers pseudomorphically grown on top of p-doped GaN as a way to reduce the specific contact resistance. The *I-V* curves of all contacts are strictly linear, indicating excellent ohmicity of the contacts. Specific contact resistances of $\rho_c = 6 \times 10^{-3}$ Ωcm^2 and $\rho_c = 1.2 \times 10^{-2}$ Ωcm^2 have been obtained for capping layer thicknesses of 2 nm and 20 nm, respectively. These results are consistent with strong band bending in the capping-layer region induced by polarization fields. As a result, the tunneling-barrier width is reduced, and the concentration of free holes increased.

REFERENCES

1. S.J. Pearton, J.C. Zolper, R.J. Shul, and F. Ren, *J. Appl. Phys.* 86, 1 (1999).
2. O. Ambacher, *J. Phys. D* 31, 2653 (1998).
3. J.-K. Ho, C.-S. Jong, C.C. Chiu, C.-N. Huang, K.-K. Shih, L-C. Chen, F.-R. Chen, and J.-J. Kai, *J. Appl. Phys.* 86, 4491 (1999).
4. Y.-L. Li, E.F. Schubert, and J.W. Graff, *Appl. Phys. Lett.* 76, 2728 (2000).
5. J.K. Sheu, G.C. Chi, and M.J. Jou, *IEEE Elec. Dev. Lett.* 22, 160 (2001).
6. S.-R. Jeon, Y.-H. Song, H.-J. Jang, G.M. Yang, S.W. Hwang, and S.J. Son, *Appl. Phys. Lett.* 78, 3265 (2001).
7. E.L. Waldron, J.W. Graff, and E.F. Schubert, *Appl. Phys. Lett.* 79, 2737 (2001).
8. O. Mayrock, H.-J. Wünsche, and F. Henneberger, *Phys. Rev. B* 62, 16870 (2000).
9. We used the PC version 10/01 of the freeware program "1D Poisson/Schrodinger" (http://www.nd.edu/~gsnider/) written by Greg Snyder, ECE-Department, University of Notre Dame, IN 46556.
10. S. Yamasaki, S. Asami, N. Shibata, M. Koike, K. Manabe, T. Tanaka, H. Amano, and I. Akasaki, *Appl. Phys. Lett.* 66, 1112 (1995).
11. A. Zubrilov, *Properties of Advanced Semiconductor Materials GaN, AlN, InN, BN, SiC, SiGe*, eds. M.E. Levinshtein, S.L. Rumyantsev, and M.S. Shur (New York: John Wiley & Sons, Inc., 2001), pp. 49–66.
12. F.F. Fang and W.E. Howard, *Phys. Rev. Lett.* 16, 797 (1966).
13. K. Kumakura, T. Makimoto, and N. Kobayashi, *Appl. Phys. Lett.* 79, 2588 (2001).